# Reaction between rare earth oxides and elemental fluorine. II. Kinetics of the fluorination of cerium dioxide*

Masayuki Takashima, Shinji Fukami,** Yoshihiro Nosaka and Terunobu Unishi
*Faculty of Engineering, Fukui University, 3-9-1 Bunkyo, Fukui-shi 910 (Japan)*

## Abstract

The reaction between cerium dioxide and fluorine gas has been studied by means of thermogravimetric, X-ray and magnetic measurements $CeO_2$ reacts with $F_2$ gas from 130 °C and converts into $CeF_3$ with a characteristic weight decrease above 270 °C. The reaction rate was found to be determined by fluorine gas diffusion described by a modified Jander equation, and the activation energy is estimated to be 80 to 90 kJ/mol Fluorine is incorporated into the crystal lattice of $CeO_2$ without change of structure or oxidation state of Ce(IV) below 270 °C To convert into $CeF_3$, the valency Ce(IV) drastically changes to Ce(III) with evolution of oxygen at 270 to 290 °C.

## Introduction

Introduction of fluorine into transition metal oxides brings about drastic changes in electric or magnetic properties [1–3]. We have recently prepared binary rare earth oxide fluorides by solid–solid reactions between rare earth oxides and fluorides and have found that these compounds have high oxide ion conductivity [4–6]. Solid–gas and solid–liquid reactions using fluorine gas or liquid HF need to be investigated to obtain a systematic view of rare earth–oxygen–fluorine systems. We have recently reported the reaction between neodymium oxide and fluorine gas [7]. As a follow-up study, our interest is focussed on the reaction between $CeO_2$ and fluorine gas. $CeO_2$ itself has been the subject of many investigations because of its high electrical conductivity [8, 9], but its reaction with fluorine gas has not yet been reported. $CeF_3$ is expected to be the final product when $CeO_2$ is treated with fluorine gas under appropriate conditions. Ce(IV) is the most stable ionic species of the oxides, while only Ce(III) of the fluorides is stable. Formation of $CeF_4$ is also expected but it seems to decompose easily by hydrolysis [10]. To solve the problems of how cerium dioxide is reduced to cerium trifluoride in oxidative fluorine gas and what the intermediate compounds are, we

---

*For Part I, see ref. 7

**Present address Onoda Cement Co Ltd., 1-1-7 Toyosu, Koutou-ku, Tokyo 135, Japan.

0022-1139/92/$5 00

have investigated the kinetics of the reaction by means of thermogravimetry, X-ray diffraction and magnetic susceptibility measurements.

## Experimental

Thermogravimetric measurements were carried out using a spring-type thermobalance (Shimadzu TGC-35) which was fluorine resistant up to 600 °C. The detectable weight change was 0.2 mg. Temperature was controlled within ± 0.2 °C at a preset temperature. Detail of the reaction apparatus has been mentioned in a previous report [7]. Fluorine gas (99% pure) was obtained from Daikin Co. and was used after removing as much HF as possible by vaporizing at $-78$ °C after liquefying at $-196$ °C. The $CeO_2$ sample was commercially available and was guaranteed 99.9% pure (from Shin-Etsu Chemical Co.). The shape, surface area and pretreatment condition of oxide samples for fluorination have been found to affect the kinetic analysis of solid–gas reactions. $CeO_2$ samples were sintered in air at 920 °C for 5 h after pelletting under a pressure of 100 kg/cm$^2$, and were then broken into coarse particles sifted out to 16 to 24 mesh. This procedure was very effective in obtaining a starting sample and increased the reproducibility. The surface area was found to be 1.3 m$^2$/g by the BET method. Products were examined by means of X-ray diffraction (Shimadzu XD-3As), fluorescent X-ray analysis (Rigaku-3030) and magnetic susceptibility analysis by using a vibrating sample magnetometer (Toei VSM-3) to clarify the reaction process.

## Results and discussion

From our previous investigation of the fluorination of rare earth oxides with $F_2$, three types of reaction were found, as shown in Fig. 1 [7]. The reaction ratio is defined as $x = 1.0$ when $CeO_2$ is completely converted into $CeF_3$. $CeO_2$ belongs to the B-group and has a critical temperature around 200 °C where the reaction occurs rapidly. Figure 2 shows the continuous tracings of change in reaction ratio as a function of temperature under fluorine pressures of 50, 100 and 150 mmHg at a rate of increase in temperature of 0.5 °C/min. Figure 3 shows those under 100 mmHg and at the temperature rates of 0.5, 1.0 and 2.0 °C/min. The reaction began to take place around 130 °C, and then a characteristic weight decrease was observed at 270 to 290 °C. Evolution of oxygen may account for this behavior. Kinetic measurements are usually conducted under constant pressures and temperatures. However, we could not obtain reproducible results because of the rapidity of the initial reaction above 200 °C while introducing fluorine gas into the reactor. Therefore, we attempted to obtain kinetic parameters such as the rate constant, activation energy and order of reaction from TG curves shown in Fig. 2. Kinetic investiga-

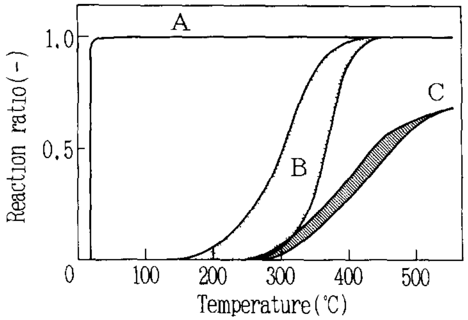

Fig 1. Three typical TG curves for the fluorination of rare earth oxides with fluorine gas under a fluorine pressure of 200 mmHg at an increase in temperature of 0 5 °C/min A group $La_2O_3$, $Pr_6O_{11}$, $Tb_4O_7$, B group $CeO_2$, $Nd_2O_3$, $Sm_2O_3$, $Eu_2O_3$, C group $Gd_2O_3$, $Dy_2O_3$, $Ho_2O_3$, $Er_2O_3$, $Tm_2O_3$, $Yb_2O_3$, $Lu_2O_3$, $Y_2O_3$

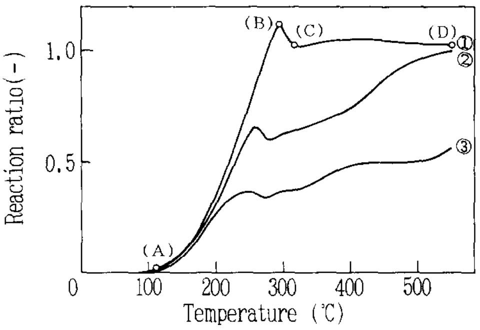

Fig 2 TG curves for the fluorination of $CeO_2$ at an increase in temperature of 0 5 °C/min under various fluorine pressures ① 150 mmHg, ② 100 mmHg, ③ 50 mmHg

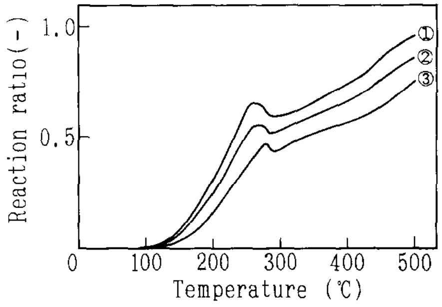

Fig 3 TG curves for the fluorination of $CeO_2$ under a fluorine pressure of 100 mmHg at various rates of increase in temperature· ① 0 5 °C/min, ② 1 0 °C/min, ③ 2 0 °C/min

tions under continuous change of temperature have rarely been found. We assume that this reaction is in the category of tarnishing reactions and that fluorine gas diffusion determines the reaction rate. The Jander equation [11] is applicable in this case. The modified Jander equation which applies to the analysis of TG data is derived as follows.

The Jander equation under the condition of gas diffusion control is expressed by

$$\frac{\mathrm{d}X}{\mathrm{d}t} = \frac{3DC(1-x)^{2/3}}{r^2\{1-(1-x)^{1/3}\}} \tag{1}$$

$$D = A\exp\left(-\frac{E_a}{RT}\right) \tag{2}$$

where $x$ = reaction ratio, $t$ = time, $T$ = temperature, $r$ = particle size, $D$ = diffusion constant, $C$ = gas concentration, $A$ = frequency factor, $E_a$ = activation energy and $R$ = gas constant. One can obtain directly from the TG curves $\mathrm{d}x/\mathrm{d}T$, not the reaction rate $\mathrm{d}x/\mathrm{d}t$. The differential of a TG curve, $\mathrm{d}x/\mathrm{d}T$, is

$$\frac{\mathrm{d}x}{\mathrm{d}T} = \frac{\mathrm{d}x}{\mathrm{d}t}\,\frac{\mathrm{d}t}{\mathrm{d}T} \tag{3}$$

Its logarithmic form is

$$\ln\frac{\mathrm{d}x}{\mathrm{d}T} = \ln\frac{\mathrm{d}x}{\mathrm{d}t} + \ln\frac{\mathrm{d}t}{\mathrm{d}T} \tag{4}$$

Equations (1), (2) and (4) lead to the Jander equation in a differential form, which is identical to eqn. (5):

$$\ln\frac{\mathrm{d}x}{\mathrm{d}T} = -\frac{E_a}{R}\,\frac{1}{T} + \ln\frac{(1-x)^{2/3}}{1-(1-x)^{1/3}} + \text{const.} \tag{5}$$

because

$$\ln\frac{\mathrm{d}t}{\mathrm{d}T} + \ln\frac{3CA}{r^2} = \text{const.} \tag{6}$$

From eqn. (5) it is clear that plots of $1/T$ *vs.* $\ln(\mathrm{d}x/\mathrm{d}T) - \ln[(1-x)^{2/3}/1-(1-x)^{1/3}]$ should result in a straight line with a slope of $-(E_a/R)$. Figures 4 and 5 show the modified Jander plots obtained from the TG curves shown in Figs. 2 and 3 They gave a reasonably straight line, which supports our approach. The activation energy $E_a$ calculated from the slope is 80 to 90 kJ/mol. This value is approximately the same as that for oxide ion diffusion in a $Y_2O_3$-doped cerium oxide [12]. This supports the analysis of the diffusion process.

Another item of interest in this study is the reaction mechanism. We studied the structural change during reaction. On the reaction path, formation of CeOF, $CeF_3$ and $CeF_4$ are presumed. The lattice constants are: $CeO_2$(cubic), $a_0 = 5.41$ Å [13]; CeOF(cubic), $a_0 = 5.70$ Å, CeOF(rhombo-

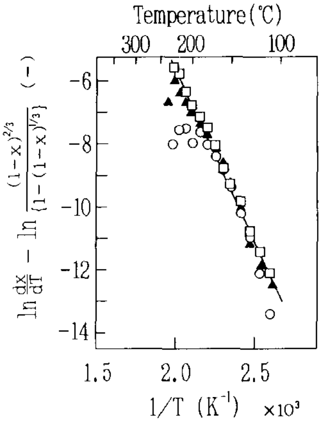

Fig 4 Modified Jander plots at an increase in temperature of 0.5 °C/min with various fluorine pressures ☐ 150 mmHg, ▲ 100 mmHg, ○ 50 mmHg

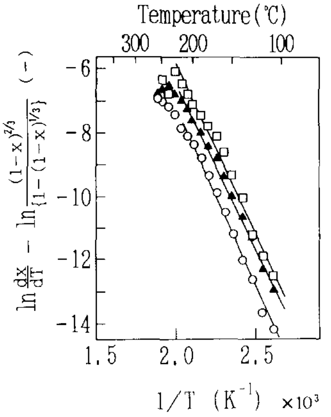

Fig 5 Modified Jander plots with a fluorine pressure of 100 mmHg at various rates of increase in temperature ☐ 0.5 °C/min, ▲ 1.0 °C/min, ○ 2.0 °C/min

hedral), $a_0 = 6.98$ Å, $\alpha = 33.56°$ [14]; $CeF_3$(hexagonal), $a_0 = 7.11$ Å, $c_0 = 7.28$ Å [15]; and $CeF_4$(monoclinic), $a_0 = 12.6$ Å, $b_0 = 10.6$ Å, $c_0 = 8.3$ Å, $\beta = 126°$ [16]. Figure 6 shows X-ray diffraction patterns for the products at A, B, C and D on the TG curve under a fluorine pressure of 150 mmHg at a rate of increase in temperature of 0.5 °C/min shown in Fig. 2.

Fluorine incorporation into the lattice should give rise to lattice expansion. The X-ray diffraction patterns of $CeO_2$ under $F_2$ remain in the cubic form without any change in lattice constant up to 270 °C. When the weight drastically decreases at 270 to 290 °C, the crystal structure suddenly changes into the hexagonal form of $CeF_3$. No diffraction line due to $CeF_4$ appears in any diffraction pattern. The fluorine content of sample D was found to be close to that of commercially available $CeF_3$ (99.9% pure)

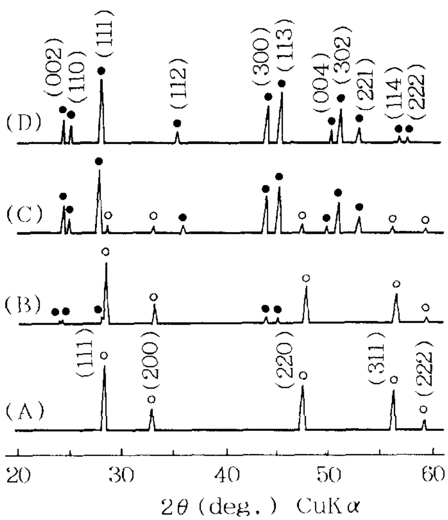

Fig 6 X-Ray diffraction patterns for products at the points A, B, C and D on the TG curve under a fluorine pressure of 150 mmHg at an increase in temperature of 0.5 C/min ○ $CeO_2$ cubic, ● $CeF_3$ (hexagonal)

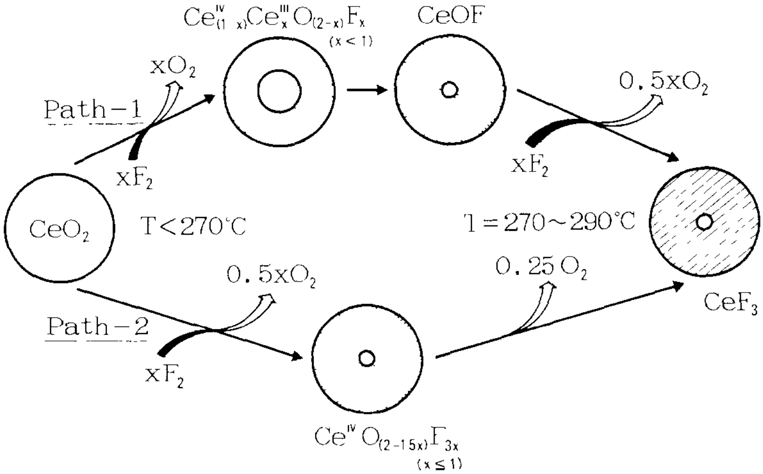

Fig 7 Reaction processes for the fluorination of $CeO_2$ with fluorine gas

by means of fluorescent X-ray analysis. This weight decrease is assumed to be due to evolution of oxygen. Two reaction paths are possible in this reaction, as illustrated in Fig. 7 In path one, two fluorine atoms substitute for two oxygen atoms, and 1 mole oxygen gas is released. Therefore, the oxidation state of cerium continuously changes to tripositive, and CeOF may be formed as an intermediate compound. On the other hand, in path two, the reaction proceeds as 1 mole of fluorine substitutes for

TABLE 1

Magnetic susceptibilities for $CeO_2$, sample B, sample C and $CeF_3$

| | $CeO_2$ | Sample B[a] | Sample C[a] | $CeF_3$ |
|---|---|---|---|---|
| Mag sus [b] | −2 33 | −3 87 | 5 66 | 7 50 |

[a] Samples B and C were obtained at points B and C on the TG curve

[b] $\times 10^6$ (EMU/Oe · g)

$\frac{1}{2}$ mole of oxygen, that is, one fluorine atom occupies one site of oxygen and another one has to be interstitial in the lattice. Therefore, the oxidation state of Ce(IV) is maintained. In this case, formation of $CeF_4$ was presumed [17], but we could not obtain any evidence of this compound. Path two seems to be preferable to explain the characteristic weight decrease that occurs at 270 to 290 °C and the reaction ratio of 1.0 at point C on the TG curve in Fig 2.

To examine this, magnetic susceptibility was measured for $CeO_2$, sample B, sample C and $CeF_3$. Samples B and C were obtained by stopping the reaction at points B and C. As listed in Table 1, the magnetic susceptibility indicates that Ce(IV) changes into Ce(III) on the change from B to C, although we have no explanation for the diamagnetic properties of $CeO_2$ and sample B. These results suggest that path two is dominant in this reaction.

## Conclusions

Cerium dioxide begins to react with fluorine gas at 130 °C and cerium trifluoride is formed with evolution of oxygen above 270 °C. Kinetically the reaction is in the category of tarnishing reactions. The Jander equation applies when considering the reaction process. The reaction rate is determined by fluorine gas diffusion. The activation energy of the diffusion process is 80 to 90 kJ/mol. Fluorine gas is incorporated into the $CeO_2$ lattice without any change of structure or oxidation state of cerium below 270 °C. Ce(IV) changes into Ce(III) at 270 to 290 °C to form $CeF_3$. No evidence for $CeF_4$ formation can be detected up to 550 °C.

## References

1 J Claverie, J Portier and P Hagenmuller, *Z. Anorg Allg Chem.*, *393* (1973) 314

2 J Ravez and M Dabadie, *Rev Chem Miner*, *10* (1973) 765

3 M Bayard, M Pouchard, P Hagenmuller and A Wold, *J Solid State Chem*, *12* (1975) 41

4 M Takashima, G Kano and H Konishi, *Nippon Kagaku Kaishi*, (1982) 1896

5 M Takashima and G Kano, *Solid State Ionics, 23* (1987) 99

6 M Takashima, G Kano, K Hirao and Y Hibino, *Nippon Kagaku Kaishi*, (1987) 1779

7 M Takashima, Y Nosaka and T Unishi, *Eur J Solid State Inorg Chem* , (1992) in press

8 T Takahashi and O Yamamoto, *Electrochem Acta, 11* (1966) 779

9 H Yahiro, Y Baba, E Eguchi and H Arai, *J Electrochem Soc* , *135* (1988) 2077

10 F H Spedding and A H Daane, *The Rare Earths*, Robert E Krieger, Huntington, NY, 1971

11 W Jander, *Z Anorg Allg Chem* , *163* (1927) 1

12 A S Nowic, D Y Wang, D S Park and J Griffith, in P Vashista, J N Mundy and G K. Shenoy (eds ), *Fast Ion Transport in Solids*, North-Holland, New York, 1979, p. 673

13 *X-Ray Powder Data File*, ASTM, No 4-0593, 1960

14 N C Baenziger, J R Holden, G E Knudson and A I Popov, *J Am Chem Soc* , *76* (1954) 4734

15 R E Thoma and G D Brunton, *Inorg Chem* , *5* (1966) 1937

16 W H Zachariasen, *Acta Crystallogr* , *2* (1949) 388

17 H von Wartenberg, *Z Anorg Allg Chem* , *244* (1940) 337